

Two Issues about the Application of V_P/V_S : Quality Improvement and Error Analysis

Duojun Zhang¹ and Larry Lines¹

¹University of Calgary, Calgary, Alberta, Canada (dazhang@ucalgary.ca)

Abstract

With the success of acquisition and processing of multiple component seismic data, people are trying to get more and better information from multicomponent seismic data to characterize the reservoir. Mapping of V_P/V_S provides important information. Due to the significant difference of frequency spectra of PP and PS seismic volumes, we designed the band pass filter based on the frequency spectrum of PS seismic volume, which has a narrower frequency band and lower dominant frequency, and applied the band pass filter to PP seismic volume. The quality of V_P/V_S map from PS and filtered PP seismic volumes was significantly improved compared with the quality of V_P/V_S map from PS and unfiltered PP seismic volumes. Meanwhile, the error from surrounding formations was analyzed because we usually cannot get reliable reflection pick from the target formation and have to interpret those coherent events from surrounding formations. The error analysis was based on the interpreted model, and the result was that the effect from surrounding formations was negligible if the velocities of surrounding formations did not change much laterally. The assumption could be satisfied in most cases when we considered the geological background. If the velocities of surrounding formations change significantly, we can limit the area to interpret the pattern of V_P/V_S to improve the reliability of this method.

Introduction

Right now, more and more people are trying to use the ratio of P-wave to S-wave velocities (V_P/V_S) from 3C/3D seismic data to monitor the recovery process of oil production or to delineate sand distribution of reservoir. The theory can be described as interpreting the reflection events from the top and bottom of target formation on PP and PS seismic volumes, calculating V_P/V_S of target formation based on equation (1):

$$\frac{V_P}{V_S} = \frac{2\Delta t_{PS} - \Delta t_{PP}}{\Delta t_{PP}} \quad (1)$$

Where Δt_{PP} is the travel time of the interpreted interval from PP sections and Δt_{PS} is the interval travel time from PS sections. Applications of this method to heavy-oil reservoirs have been shown by Watson et al. (2002) and Lines et al. (2005).

Generally, there is a big difference between the frequency spectra of PP and PS seismic volumes. In the depth of target formation, the frequency band of PP spectrum is wider than that of the PS spectrum and the dominant frequency of PP data is much higher. This fact will have a negative effect on the calculated V_P/V_S from interpreted interval. Also in the practice, it is difficult to resolve reflections from the top and bottom of the target layer in the real seismic data. The reflected events from the top and bottom of the pay zone are often incoherent and difficult to pick, we will have to select the reference top and bottom horizons from above and below our target formation to pick, which

surround our target formation, the calculated V_P/V_S will be smeared or affected by its surrounding layers. In this case, the error of V_P/V_S from surrounding formations should be analyzed to implement the application of V_P/V_S correctly.

In this paper, we introduced one method to get rid of the negative effect from the difference of frequency spectra to improve the quality of V_P/V_S map. Error analysis was discussed and the result demonstrated that the effect from surrounding formations would not erode the usability of V_P/V_S map if V_P/V_S of the surrounding formations did not change much laterally.

Quality Improvement

As previously mentioned, the frequency spectra of PP and PS seismic volumes in the depth of our target formation are quite different (Figure 1). The frequency band of PP spectrum is wider than that of the PS spectrum and the dominant frequency of PP data is much higher. To solve the problem, we designed a band pass filter (0, 10, 30, 55Hz) based on the amplitude spectrum of PS seismic volume, and applied the designed band pass filter to PP seismic data. Comparing unfiltered PP data with filtered PP data (Figure 2), we can see the difference of event character between them, two closely distributed events with higher frequency on the unfiltered PP data became to be one event with lower frequency on filtered PP data, which is selected as reference top horizon.

Figures 3 and 4 are the final maps of V_P/V_S between the interpreted reference top and bottom horizons. Yellow, orange and red colors show lower V_P/V_S , most probably deduced by heavy-oil cold production. The values of V_P/V_S around production wells are generally lower than elsewhere. The lower values of V_P/V_S have a good correspondence with well locations in both maps, but the map from filtered PP and PS data has a higher lateral resolution and better correspondence with well locations, especially in the west-center part. This result suggests the importance of the poststack processing of the seismic volume to enhance the similarity between PP and PS seismic volumes.

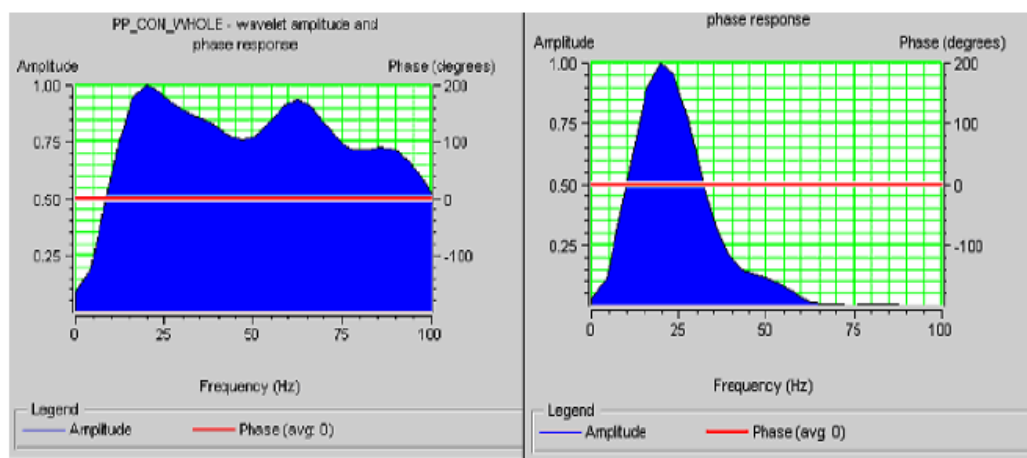


Figure 1. Amplitude spectra of wavelets extracted from PP (left) and PS (right) seismic data.

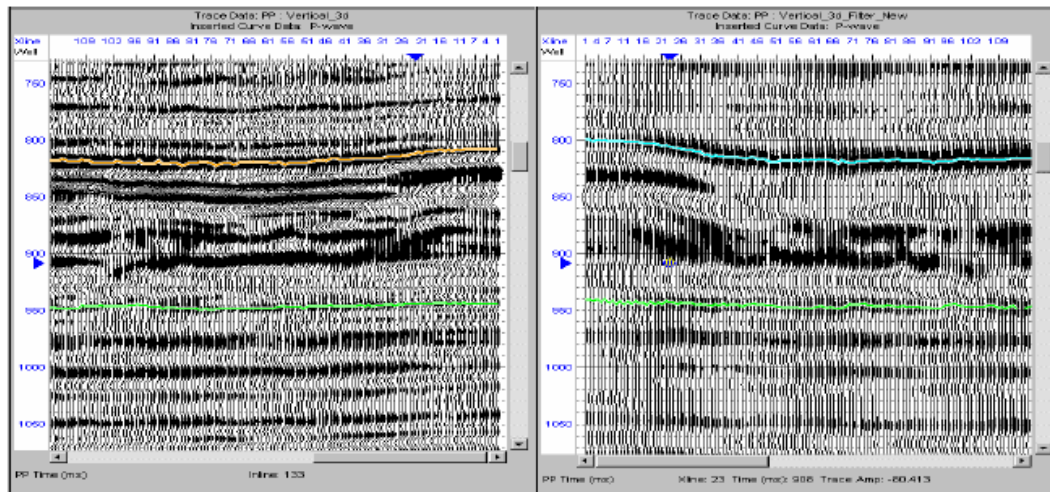


Figure 2. Comparison between unfiltered PP (left) and filtered PP (right) seismic data.

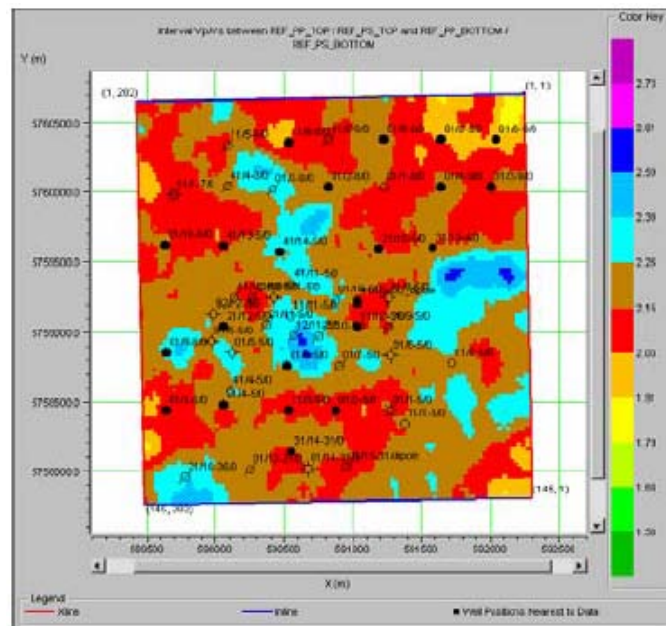


Figure 3. V_p/V_s between top and bottom horizons from unfiltered PP and PS data.

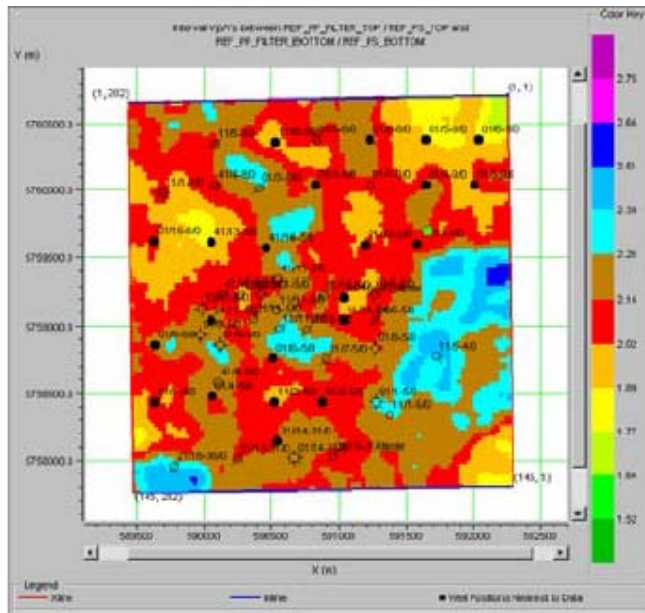


Figure 4. V_p/V_s between top and bottom horizons from filtered PP and PS data.

Error Analysis

Figure 5 is the sketch of the interpreted model of PP and PS data, where V_{P1} , V_P , and V_{P2} are P-wave velocities of surrounding and target formations, V_{S1} , V_S , and V_{S2} are S-wave velocities of surrounding and target formations, Δt_{PP1} , Δt_{PP} and Δt_{PP2} are interpreted travel times of surrounding and target formations from PP seismic data, Δt_{PS1} , Δt_{PS} and Δt_{PS2} are interpreted travel times of surrounding and target formations from PS seismic data, Δd_1 , Δd and Δd_2 are the thickness of surrounding and target formations.

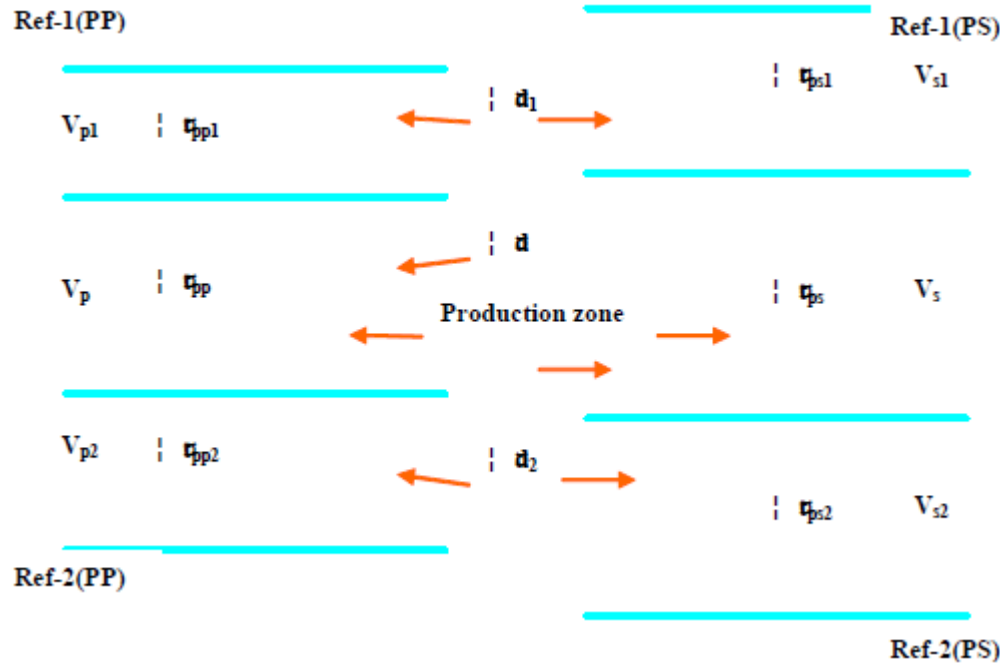


Figure 5. The sketch of interpreted model.

To simplify the derivation, we assume that $C_{S1}=\Delta t_{PS1}/\Delta t_{PS}$, $C_{S2}=\Delta t_{PS2}/\Delta t_{PS}$, $C_{P1}=\Delta t_{PP1}/\Delta t_{PP}$, $C_{P2}=\Delta t_{PP2}/\Delta t_{PP}$, which mean that C_{S1} , C_{S2} , C_{P1} and C_{P2} are the ratios of travel times for surrounding layers to reservoir zones. We also assume that $\Delta T_{PS}=\Delta t_{PS1}+\Delta t_{PS}+\Delta t_{PS2}$, $\Delta T_{PP}=\Delta t_{PP1}+\Delta t_{PP}+\Delta t_{PP2}$, $r_1=V_{P1}/V_{S1}$, $r=V_P/V_S$, $r_2=V_{P2}/V_{S2}$, V_P^* is the average velocity of the P-wave between the interpreted interval and V_S^* is the average velocity of the S-wave between the interpreted interval, then the ratio of V_P^* and V_S^* can be expressed as:

$$\begin{aligned}
 R &= \frac{V_P^*}{V_S^*} = \frac{2\Delta T_{PS}}{\Delta T_{PP}} - 1 = \frac{2(\Delta t_{PS1} + \Delta t_{PS} + \Delta t_{PS2})}{\Delta t_{PP1} + \Delta t_{PP} + \Delta t_{PP2}} - 1 \\
 &= \frac{\frac{r_1+1}{r+1}C_{P1} + \frac{r_2+1}{r+1}C_{P2} + 1}{C_{P1} + C_{P2} + 1} \cdot \frac{V_P}{V_S} + \frac{\frac{r_1+1}{r+1}C_{P1} + \frac{r_2+1}{r+1}C_{P2} - (C_{P1} + C_{P2})}{C_{P1} + C_{P2} + 1} \quad (2)
 \end{aligned}$$

If $r_1 \approx r_2 \approx 2$, then:

$$R \approx 2 + \frac{r-2}{C_{P1} + C_{P2} + 1} \quad (3)$$

Assume $\Delta d_1/\Delta d \approx 1$ and $\Delta d_2/\Delta d \approx 1$, then:

$$C_{P1} = \frac{\Delta d_1}{\Delta d} \frac{V_P}{V_{P1}} \approx \frac{V_P}{V_{P1}}, \quad C_{P2} = \frac{\Delta d_2}{\Delta d} \frac{V_P}{V_{P2}} \approx \frac{V_P}{V_{P2}};$$

$$R \approx 2 + \frac{r-2}{\frac{V_P}{V_{P1}} + \frac{V_P}{V_{P2}} + 1} \quad (4)$$

If we assume $V_{P1} \approx V_{P2}$, then:

$$R \approx 2 + \frac{r-2}{2\frac{V_P}{V_{P1}} + 1} = 2 + \frac{r-2}{2r_p + 1} \quad (5)$$

where $r_p = V_P/V_{P1}$. The error will be:

$$E = R - r = (2-r) \frac{2r_p}{2r_p + 1} \quad (6)$$

The equation of error can be divided into two parts: one is $(2-r)$, another is $2r_p/(2r_p+1)$. The first part represents the ratio difference between the production zone and surrounding zone, and 2 is due to our assumption that $r_1 \approx r_2 \approx 2.0$, and the value of this part is the basic element of the error. The second part is actually the coefficient that is due to the difference of the P-wave velocity between the production zone and surrounding zone. Since both r and r_p vary laterally, the error will be variable laterally.

We assume that: $V_S \approx V_{S1} \approx V_{S2} \approx 1500$ m/s (since velocity of S-wave does not change dramatically due to production), $V_{P1} \approx V_{P2} \approx 3000$ m/s, based on the above two equations of R and E , the following sheet and graphs are generated (Table 1). From the sheet and graphs, we can conclude that: if V_{P1}/V_{S1} and V_{P2}/V_{S2} do not change laterally, R will keep the similar pattern with the ratio r of the production zone; but the error will increase with the increasing velocity difference between the production zone and surrounding zone. On the other side, if V_{P1}/V_{S1} and V_{P2}/V_{S2} change dramatically laterally, then R will probably reach a different pattern compared with r . Thus, generally, we should interpret the reference horizons as close as possible to the top and bottom of the production zone to reduce the effect of the surrounding zone to the least.

In most cases, the production formation is surrounded by formations with the lithology of shale, which acts as seal or resource, or both. Shale is usually deposited in a deep-water environment with less energy and the velocity performs little change laterally. At the same time, the reflection events from shaly formation are usually coherent; they are good candidates for reference horizons. Both of the above facts provide a

good condition for us to get a calculated V_P^*/V_S^* map from interpreted interval, which will have a similar pattern with the V_P/V_S map of target formation.

On the other hand, if the velocities of surrounding formations have a lateral dramatic change due to fault or depositional environment, we can analyze the pattern of calculated V_P^*/V_S^* in restricted area, where the velocities of surrounding formations are relatively stable, to improve the reliability of this method.

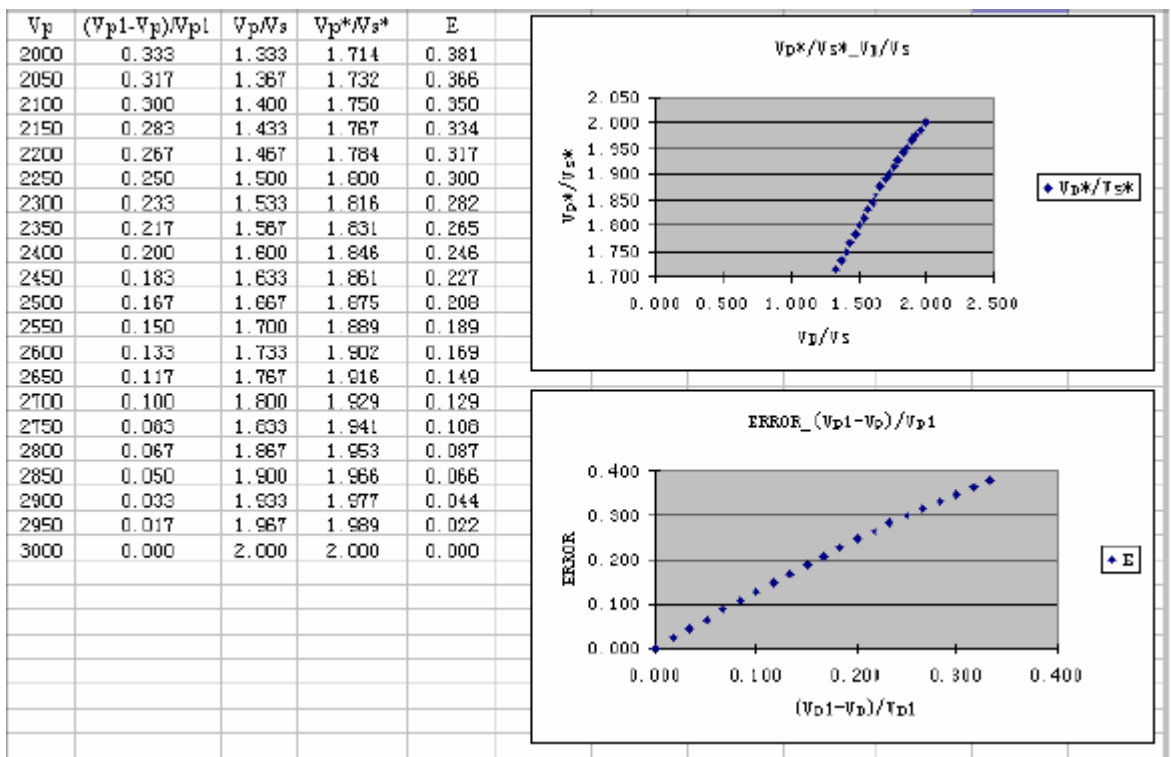


Table 1. The result of error analysis.

Conclusions

From above analysis, we can conclude that post-stack processing of the PP seismic volume to enhance the similarity between PP and PS seismic volumes will generally help us get a more reasonable result. If the velocities of the surrounding formations do not change much laterally, the calculated V_P^*/V_S^* from the interpreted interval will have a similar pattern with the V_P/V_S map of target formation.

Acknowledgements

We would like to thank Joan Embleton, Kevin Hall, Rolf Maier, Richard Xu and Bruce Palmiere for their support and technical discussions. I am also grateful to the sponsors for their support to the CREWES and CHORUS projects.

References Cited

- Chen, S., L. Lines, J. Embleton, P.F. Daley, and L. Mayo, 2003, Seismic detection of cold production footprints of heavy oil in Lloydminster field: the CSEG convention, June, Calgary, Alberta, Canada.
- Lines, L., S. Chen, P.F. Daley, J. Embleton, and L. Mayo, 2003, Seismic pursuit of wormholes: *The Leading Edge*, v. 22, p. 459-461.
- Lines, L.R., Y. Zou, D.A. Zhang, K. Hall, J. Embleton, B. Palmiere, C. Reine, P. Bessette, P. Cary, and D. Secord, 2005, Vp/Vs characterization of a heavy-oil reservoir: *The Leading Edge*, v. 24.
- Murphy, W., A. Reischer, and K. Hsu, 1993, Modulus decomposition of compressional and shear velocities in sand bodies: *Geophysics*, v. 58, p. 227-239.
- Sawatzky, R.P., D.A. Lillico, M.J. London, B.R. Tremblay, and R.M. Coates, 2002, Tracking cold production footprints: CIPC conference, Calgary, Alberta, Canada.
- Watson, I.A., L.R. Lines, and K.F. Brittle, 2002, Heavy-oil reservoir characterization using elastic wave properties: *The Leading Edge*, v. 21, p. 736-739.